7

Keratin-based Nanofibres

Claudio Tonin, Annalisa Aluigi, Alessio Varesano and Claudia Vineis
ISMAC, Institute for Macromolecular Studies, CNR, National Research Council
Italy

1. Introduction

The interest in biopolymers from renewable resources as alternatives to polymers made from oil and other fossil resources has been increasing over the years. Biopolymers are also considered environmentally friendly over their entire live-cycle. There is much recent literature on carbohydrates and proteins derived from plants and animals and polyesters made from the fermentation of plant material. As to whether it is ethically justifiable to convert valuable foodstuffs into commodities is open to question. The focus here is on keratin, one of the most abundant and mostly unexploited non-food proteins, being the major component of hair, feathers, nails and horns of mammals and birds. In spite of their important and interesting characteristics keratin wastes represent a rather complicated disposal challenge because burning for fuel is inefficient and polluting due to the high sulphur content (3-4% wt). The total amount of keratin (including fibre by-products from the wool textile industry, poor quality raw wools from farms and butchery waste) has been estimated worldwide at more than 5 million tonnes per year (Barone et al., 2005). Ground horn and nail is used as a nitrogenous fertilizer for gardening and, more recently, has been processed by caustic hydrolysis to produce biodegradable surfactants for fire extinguisher foams. However, most keratin wastes made from unserviceable wools and feathers from poultry are not valorised and are simply disposed of (Martínez-Hernández et al., 2007; Schmidt, 1998). Pooling and processing into biopolymers might be a better way of exploiting such a large quantity of protein biomass. Keratin-based materials can be used in biotechnological and biomedical fields for tissue engineering and the production of affinity membranes, due to their biocompatibility, their ability to support fibroblast growth and absorb heavy metal ions and volatile organic compounds (VOCs). Transforming keratin into nanofibres by electrospinning combines the aforementioned properties of keratin with the high surface to volume ratio and the high porosity of nano-structured textiles. This may be an original and promising approach for the fabrication of scaffolds for tissue engineering and filtration devices.

Keratin distinguishes itself from other structural proteins by the quantity of cysteine residues in the protein molecules (7-20% of the total amino acid residues). In particular, cysteine amino acids form inter and intra molecular disulphide bonds (cysteine residues) giving rise to a compact three-dimensional structure that confers a high stability to the protein (Dowling et al., 1986).

Because of their low molecular weight (9–60 kDa), keratin-based materials have poor mechanical properties. Moreover, like most natural polymers, keratin is not thermoplastic. For electrospinning keratin should be blended with suitable polymers using common,

Source: Nanofibers, Book edited by: Ashok Kumar,
ISBN 978-953-7619-86-2, pp. 438, February 2010, INTECH, Croatia, downloaded from SCIYO.COM

volatile and easy to handle solvents. This is also recommended when mechanical performance is needed (Aluigi et al., 2008; Katoh et al., 2004; Zoccola et al., 2008). This chapter describes the extraction of keratin from wool and electrospinning of keratin-based blends with high molecular weight polymers. Blends of keratin with poly(ethylene-oxide) (PEO) and fibroin are suitable for biomedical application (tissue engineering and medical textiles), while keratin/polyamide 6 (PA6) nanofibres can be used for active filtration of air and water.

2. Keratin and regenerated keratin

Keratins represent a group of fibrous proteins with high sulphur content produced in some epithelial cells of vertebrate such as reptiles, birds and mammals. In particular, the cysteine amino acid residues form inter and intra molecular disulphide bonds (cystine residues) that give rise to a compact three-dimensional structure that confers to keratin proteins a high resistance to chemical and enzymatic attacks (Dowling et al., 1986). There are two kinds of keratins: the "hard-keratin" and the "soft-keratin" according to the physical and chemical properties, particularly the sulphur content. Soft keratins, with a sulphur content <3% wt, are found in the *stratum corneum* of the skin whereas the hard keratins found in hair, wool, feather, nails and horns and have a sulphur content > 3% wt (Fraser et al., 1972). A further classification is based on the X-ray diffraction pattern obtained from different keratin proteins. The α-helix appears to be the basic fibrillar element in all soft keratins and in the hard keratins from mammals (Crick, 1953). Studies carried out on the structure of feather keratin have shown that about 28% of the protein molecule has a β-conformation; the remainder does not possess a geometrically regular secondary structure (Fraser et al., 1971).
A key problem in blending keratin with other polymers is to find a suitable solvent capable of dissolving the complicated structure of the protein. Generally a mixture of solvent systems in which different components have different functions is used, one component breaks the hydrogen bonds while the reducing or oxidising agent breaks the disulphide bonds. Some multiple solvent systems that have been utilized are: urea/reducing agent (Yamauchi et al., 1996), carbamide/H_2O_2/H_2O and carbamide/2-mercaptoethanol (Garret & Grisham, 2002), or Cu-oxam metal complex system ([$Cu(NH_3)4(OH)_2$]) (Aluigi et al., 2004). In 2005, Xie and co-workers tested ionic liquids, particularly 1-butyl-3-methyllimidazolium-chloride ($BMIM^+Cl^-$), as a solvent for keratin proteins (Xie et al., 2005).
Recently, two chemical-free processes using just water and heat had been explored as methods of dissolving and converting keratinous materials (i.e. wool and feathers, respectively) : steam explosion (Tonin et al., 2006) and superheated water (Yin et al., 2007). Steam explosion is based on short time steam cooking of biomasses at a high temperature for several minutes, followed by explosive decompression. Using saturated steam at 220°C (~22 bar) for 10 min followed by a rapid decompression, wool fibres were disrupted into solid and liquid phases consisting of oligo-peptides, water-soluble peptides and free amino acids (Tonin et al., 2006). The second process consisted of treating feather barbs with superheated water at ~220°C and ~22 bar for 2 h followed by cooling. Most of the keratin was converted into oligo-peptides with a molecular weight of about 1.0 and 1.8 kDa (Yin et al., 2007).
However, for the electrospinning process, volatile and easy to handle solvents are needed and for this reason we have studied the solvation properties of water and formic acid for keratin.

2.1 Wool keratin

Wool fibre is a complex multi-cell system composed of inanimate cells which differ in composition, morphology and properties. The principal component of wool fibres is keratin and there is also a small amount of lipids (0.1%) and mineral salts (0.5%). Wool cleaning for scientific purposes is carried out by means of extraction with petroleum ether, ethanol and water (von Bergen, 1963).

The disulphide bonds of cystine form both inter and intra chain cross-links and are responsible for the greater stability and lower solubility of keratin compared with most proteins. Therefore, the presence of cystine plays the most important role in the chemical, thermal and mechanical properties of wool. Although disulphide bonds are responsible for keratin reticulation in wool, there are other different kinds of cross-links: hydrophobic bonds occur between non polar groups; hydrogen bonds have a very important influence on the mechanical properties of the wool fibre; ionic bonds occur between carboxylic anions and ammonium cations. These ionic bonds depend on the pH of the environment. In fact, at the isoelectric point (pH=4.9), the quantity of ionic bonds is greatest because the protein exists as zwitterions ($^{+}H3N—CHR—COO^{-}$). When the pH is very acid or very basic, there is a reduction in the number of ionic bonds. At low pH values the COO^{-} groups are protonated, while at high levels the $NH3^{+}$ groups are deprotonated. (von Bergen, 1963).

Proteins extracted from wool can be separated into four different groups: the low sulphur content keratins (LS) that have a molecular weight between 45 and 60 kDa; the high sulphur content keratins (HS) with a molecular weight of between 11 and 28 kDa and the high-glycine and tyrosine content proteins with a molecular weight of between 9 and 12 kDa (Jeffrey, P. D., 1972). The low sulphur content proteins have an α-helical crystalline structure (α-keratins), while the other proteins do not have a helicoidal structure.

X-ray studies showed that the secondary structure of α-keratins is dextrorotatory helicoidal. This α-helix is stabilized by the presence of hydrogen bonds between the N-H group of a peptide bond and the carbonyl group of a peptide bond placed over four residues. Although the strength of a single hydrogen bond (~5 kcal/mole) is only 5% of that of C-C and C-H covalent bonds the large number of hydrogen bonds confers a remarkable stability to the α-helix crystallites. The conformation of the α-helix is characteristic for the wool fibre in its natural state, therefore it is found in the fibre which is not stretched along its axis (Pauling & Corey, 1953). During stretching, the α-helix declines and β-keratin appears (Tonin et al., 2004).

2.2 Preparation and characterization of keratin solutions

Keratin extraction from wool may take place only after the reduction or oxidation of disulphide bonds. The reducing agents often used are thiols (thioglycolic acid, dithiothreitol and 2-mercaptoethanol) while oxidizing agents are peracetic or performic acids (Yamauchi et al., 1996; Thompson & O'Donnel, 1959). All these agents are always used in combination with protein denaturing agent (e.g. urea) that breaks hydrogen bonds and extraction yields range from 50 to 70% wt. However, for further scaled-up processes, we preferred to use sulphitolysis reaction, although the extraction yield is lower (37% wt), instead of harmful reducing and oxidizing agents. The sulphitolysis is a reaction of wool with sulphite ions that break disulphide bonds in thiols and S-sulphonate anions, known as Bunte salts (Cecil, 1963).

Five grams of cleaned fibres were cut into snippets and put in 100 ml of aqueous solution containing urea (8 M), m-bisulphite 0.5 M, adjusted to pH 6.5 with NaOH 5 N and treated

by shaking for 2 h at 65°C. Successively, the solution was filtered through a 5 μm pore-size filter using a vacuum pump and then dialyzed against distilled water using cellulose tubes (molecular mass cut-off 12000-14000) for three days, changing the outer solution four times a day. The dialyzed part was first concentrated with a rotary vacuum evaporator in order to prepare solutions at different keratin concentrations (0.5, 1.5, 3.5 and 5% wt). The solution at 5%wt was cast onto a polyester plate and dried at 50°C overnight in order to prepare keratin films regenerated from water (samples labelled as KW). A part of keratin regenerated from water was dissolved in formic acid for 4h, so as to have solutions at different keratin concentrations (0.5, 1.5, 3.5 and 5% wt). The solution of keratin in formic acid at 5% wt was cast onto polyester plates and dried at 50°C overnight in order to prepare keratin films regenerated from water (samples labelled as KF).

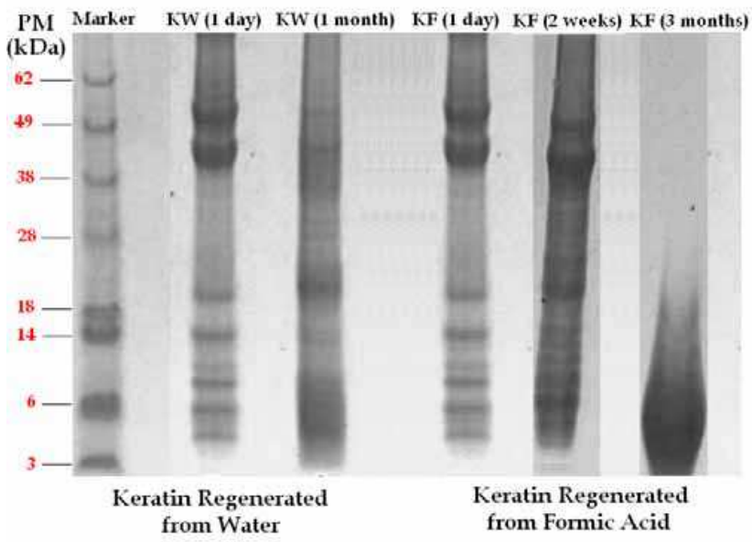

Fig. 1. SDS-PAGE of KW and KF.

The stability of keratin dissolved in water and in formic acid solutions was studied both following the protein degradation during time and the flocculation process by turbidity measurements. The molecular weight distribution analysis conducted by electrophoresis SDS-PAGE (reported in Fig. 1), revealed that the keratin regenerated from a one month old aqueous solution was degraded, in fact the high molecular weight proteins (at 45 and 60 kDa) disappear, while a series of proteins having molecular weights below 38 kDa appear. Regarding keratin in a formic acid solution, the keratin regenerated from a fresh solution (1 day) is not degraded while a slight degradation appears after two weeks and after three months there is a complete digestion of the protein.

Turbidity (τ) of solutions was calculated by measuring the transmittance T at 540 nm using the following Eq. 1:

$$\tau = -(\ln T) / c \tag{1}$$

where c is the cell length (1cm).

Fig. 2 shows that turbidity of the keratin aqueous solution increases with the increase in the keratin concentration, suggesting that higher concentrations promote protein chain aggregation (flocculation). On the other hand the turbidity of keratin dissolved in formic

acid remains unchanged with increasing keratin concentration, indicating that flocculation does not occur, at least over a certain range of keratin concentration.

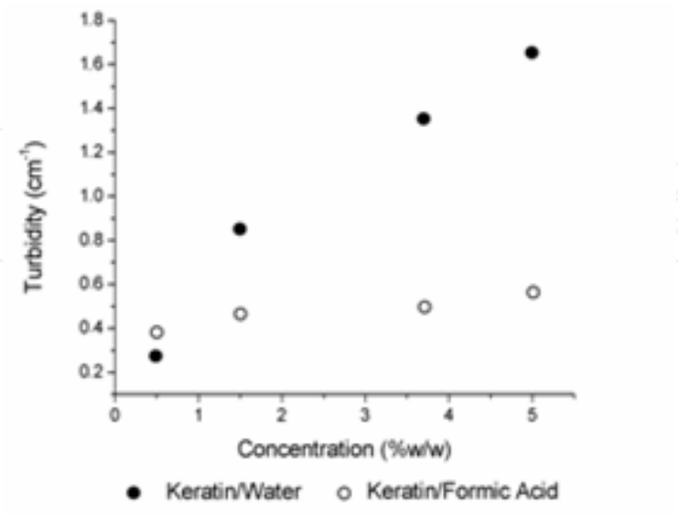

Fig. 2. Turbidity of keratin dissolved in water and in formic acid

Viscosities of the keratin solutions at 5% wt, were plotted against the shear rate (Fig. 3). In the whole shear range investigated, the viscosity of keratin dissolved in formic acid was higher than that of keratin in water. This behaviour indicates that formic acid has better solvation properties for keratin than water. This is because formic acid is more polar than water and forms strong interactions with the polar side chain groups of keratin such as CO, OH, COOH and NH_3^+. As a consequence, the molecular chains become closer in formic acid than in water and this is confirmed by the lower turbidity.

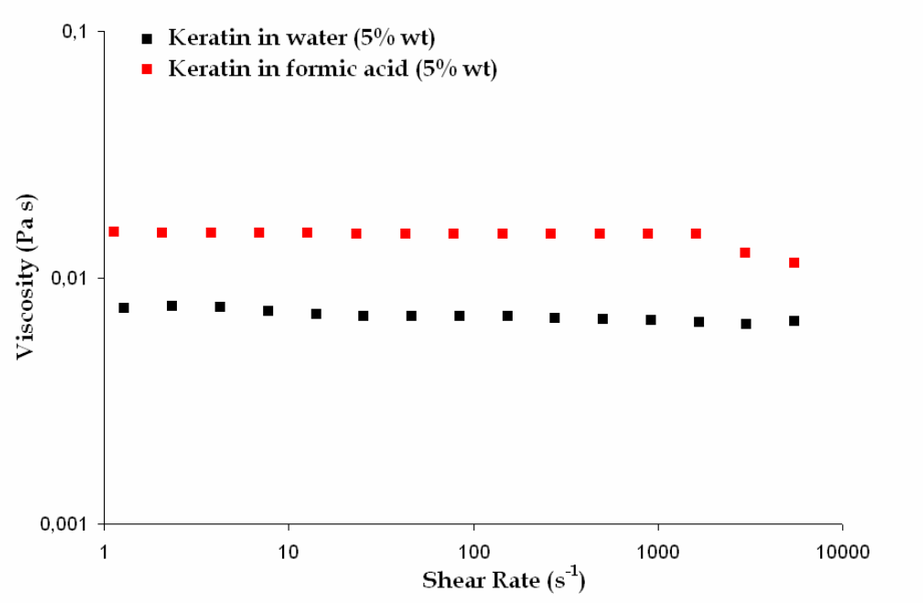

Fig. 3. Rheological behaviour of the keratin in water and keratin in formic acid solutions

3. Electrospinning

Several methods are dedicated to producing small diameter fibres for high-volume production such as fibrillation (Homonoff, 2008; Perez et al., 2000), island-in-sea (Pourdeyhimi et al., 2006), and a novel melt-blowing system (Bryner & Armantrout, 2006; Ellison et al., 2007); or highly accurate methods such as nanolithography (Tseng et al., 2005; Xie et al., 2006) and self-assembly (Zhang, 2002). However, their usefulness is restricted by combinations of narrow material ranges, high costs and low production rates. In comparison, electrospinning is a simple and low cost process, and has an intermediate production rate (Ramakrishna et al., 2006).

Electrospinning is a physical phenomenon classified as a branch of electro-fluid-dynamics. The process is based on the electrostatic repulsion of charges ruled by the well-known Coulomb law. By means of an electrostatic field, an electrospinning apparatus generates electrically-driven polymer jets that solidify into sub-micron scale polymer-based filaments (usually called nanofibres). The idea was patented in the early 20th century (Cooley, 1902; Morton, 1902; Formhals, 1934); however, the invention was disregarded until the 1990s (Huang et al., 2003; Li & Xia, 2004), probably due to lack of knowledge and interest of both industries and scientists about tiny fibres. Electrospinning works with polymer melts and polymer solutions, but few research papers deal with electrospinning of molten polymer (so-called "melt-electrospinning") compared with the huge literature regarding electrospinning of polymer solutions (usually simply referred to as "electrospinning").

Electrospinning can be usefully employed in a wide range of applications requiring sub-micron scale fibre diameter such as: filtration (Tsai et al., 2002; Qin & Wang, 2006; Li et al., 2006; Barhate & Ramakrishna, 2007), membrane separation (Shin et al., 2005; Gopal et al., 2006), protective clothing and breathable garments (Gibson et al., 2001), wound dressings and scaffolds for tissue engineering (Pham et al., 2006; Lee et al., 2008; Sill & von Recum, 2008), and drug delivery (Sill & von Recum, 2008).

A basic electrospinning setup consists of three elements: an electrical generator (high voltage supply), a capillary (jet source) and a metal collector (target). The solution is usually electrically charged by the generator and the collector is grounded, but it is also possible to invert the system by electrically charging the collector and grounding the solution (Kilic et al., 2008). A scheme of an electrospinning apparatus is shown in Fig. 4.

A pump pushes the polymer solution through the capillary with a fixed flow rate by means of a syringe. The generator, connected by a wire to the metal tip of the capillary, supplies the

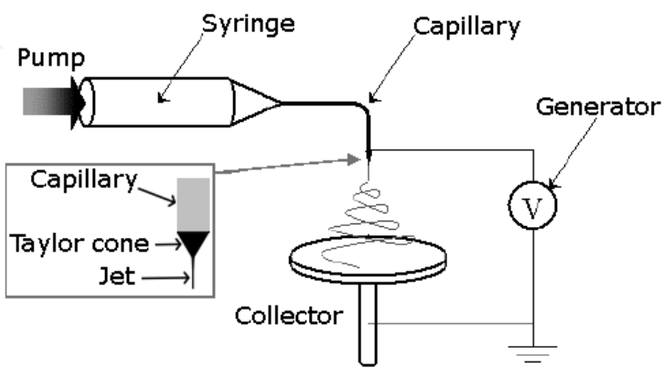

Fig. 4. Scheme of an electrospinning setup. In the box: enlargement of the capillary tip.

voltage to the solution. A stream of solution (jet) is produced from the tip toward the grounded metal collector on which electrospun nanofibres were collected. Usually, the production rate of a single jet is less than 10 g h^{-1} of nanofibres (Tsai et al., 2002), depending on polymer concentration and process conditions, mainly the flow rate of solution.

The electrospinning process starts when the voltage generator is turned on. The electrical potential of the droplet surface at the capillary tip is increased to a sufficiently high value that causes the droplet to assume a steady conical shape, known as the Taylor cone (see box in Fig. 4), instead of a spherical shape. The electrostatic forces act in opposition to the surface tension of the fluid. The Coulomb repulsion between the charges promotes the formation of the cone; on the opposite the surface tension of the fluid favours sphere-like shapes. As the electrostatic forces exceed the surface tension, a charged jet of fluid is ejected from the vertex of the cone (Yarin et al., 2001; Shin et al., 2001).

The trajectory of the jet solution begins with a straight segment. The diameter of the jet is one or two orders of magnitude smaller that the inner diameter of the capillary from which the jet is generated, and progressively decreases during its journey towards the collector. The diameter reduction occurs thank to two mechanisms: (*a*) the electrostatic repulsion forces of the charges in the jet tend to extend the jet itself, and (*b*) the solvent evaporation leaves the solid materials in the jet (e.g. polymer), this effect is self-induced because as the diameter decreases the evaporation further increases. Moreover, it worth noting that as the solvent evaporates the concentration and the viscoelastic properties of the liquid jet change.

After the straight segment, the jet is subjected to a bending instability and its trajectory becomes disordered; the oscillation eventually evolves into a spiral, similar to the movement of a whip (so-called whipping motion), as illustrated in Fig. 4. Finally, the jet completely solidifies into a nanofibre and deposits on the collector as a disordered continuous filament (non-woven structure). In spite of the ease of the electrospinning, the onset of bending instability is quite a complex problem; several theories and mechanisms have been recently proposed to explain this phenomenon (Shin et al., 2001; Deitzel et al., 2001; Reneker & Yarin, 2008).

The fibre-forming process depends on operating parameters (applied voltage, working distance between tip and collector, flow-rate of solution, tip diameter), properties of the polymer solution (polymer molecular weight, concentration, relaxation time, viscosity, electrical conductivity, surface tension, and vapour tension of the solvent), and environmental parameters such as temperature, humidity and ventilation (Theron et al., 2004). Depending on working conditions and polymer solution properties, the electrospun jet might be subjected to many phenomena such as branching, splitting, buckling, jet break-up (spraying), production of flat ribbon or beaded nanofibres that engenders different morphologies (Reneker & Yarin, 2008).

4. Keratin/PEO blend nanofibres

Recently in a leading opinion paper, Furth and co-workers (Furth et al., 2007) stated that they had been investigating the utility of keratin-based biomaterials for regenerative medicine applications. Keratin contains intrinsic sites of cellular recognition that mimic the extra-cellular matrix and keratin-based biomaterials demonstrated cell instructive capabilities. Certain keratin materials have been shown to be mitogenic and chemotactic for a variety of cell types, and to mediate changes in gene expression consistent with the promotion of wound healing. Moreover, other recent works (Tachinaba et al., 2002;

Tachinaba et al., 2005; Hamasaki et al., 2008) have highlighted the excellent cell adhesion onto wool keratin sponges produced by lyophilisation from aqueous solution. These results show that keratin is a useful biomaterial for scaffolds for cell cultivation.
The poor mechanical properties of regenerated keratin hinder its processability and restrict its practical applications to blends with appropriate polymers with better structural properties. Our attempts to obtain filaments of pure regenerated keratin from water were indeed unsuccessful; moreover, literature reports on the fabrication of regenerated keratin films (Tanabe et al., 2004) using cross linking agents, and the fabrication of composite nanofibres of regenerated silk fibroin blended with synthetic polymers such as poly(ethylene oxide) (PEO) (Jin et al., 2002). PEO is an amphiphilic water soluble and non-degradable polymer, with good biocompatibility (Desai & Hubbel, 1991) and low toxicity (Bergsma et al., 1995). This polymer is often used as an ideal model for the electrospinning process (Theron et al., 2004; Son et al., 2004) because it can be electrospun without defects from aqueous solutions in a rather narrow range of conditions.
We studied the production and the characterization of nanofibres produced by electrospinning of pure PEO and 50/50 wt/wt keratin/PEO blends, from aqueous solution of the polymers, in different operating conditions. The nanofibres were studied by Scanning Electron Microscopy (SEM) and Differential Scanning Calorimetry (DSC). The results were compared with those obtained by thin films produced by casting from the same solutions, with the aim of investigating the influence of the production processes on the structural arrangement of these materials.

4.1 Materials and methods

Keratin was obtained from wool by means of a sulphitolysis extraction method. PEO powder with an average molecular weight of 4×10^5 g mol^{-1} was dissolved in distilled water at ambient temperature for about 12 h. The concentrations used were 5, 7 and 10 % wt.
The keratin/PEO blend solutions were prepared at room temperature in about 12 h by simply adding PEO powder to the keratin aqueous solution. The solutions of keratin/PEO blend had total polymer concentrations of 5, 7 and 10 % wt with a keratin/PEO weight ratio of 50/50. These solutions were electrospun at 20 cm working distance to ensure that the nanofibres were dried. The applied voltages were between 10 and 30 kV. The process was stopped after about 10 minutes. During the electrospinning process, environmental conditions were kept in check; in particular, the temperature was from 20 to 25 °C and the relative humidity was in the range 55-65 %.

4.2 Solution characterization

Viscosity is an important factor for complete fibre formation in the electrospinning of polymer solutions. In particular, fibres without beads were produced when polymer chain entanglements are present at sufficient concentration (Shenoy et al., 2005). Moreover, fibre formation is promoted at low polymer concentrations, increasing solution conductivity (Son et al., 2004).
A great increase in conductivity was measured from solutions containing the keratin because of SDS that remains associated with keratin through ionic interaction conferring negative charges to the protein (Schrooyen et al., 2001). In fact the conductivity of pure PEO was about 0.120 mS cm^{-1} and the conductivity of keratin/PEO was 1.282 mS cm^{-1} (at polymer concentration 7% wt).

Fig. 5 shows the flow curves of PEO and keratin/PEO solutions at 5, 7 and 10% wt of polymers in water. All solutions behave like shear-thinning fluids. At low shear rates, disentanglement is balanced by formation of new entanglements, thus the fluid has a Newtonian behaviour which corresponds to a constant viscosity value (zero-shear viscosity). At higher values of shear rate, the disentanglement rate exceeds the rate of entanglement formation, therefore the viscosity decreases and shear-thinning behaviour is observed. The onset of shear thinning shifts to lower values of shear rate with the increase of polymer concentrations for both pure PEO and keratin/PEO solutions. The zero-shear viscosity increases when the polymer concentration increases. It is worth nothing that the keratin/PEO solutions at concentrations of 7 and 10% wt show flow curves Comparable with 5 and 7% PEO solutions, respectively. Thus, the keratin with a relatively low molecular weight slightly increases the viscosities of the keratin/PEO solutions, but its contribution is not negligible (Varesano et al., 2008).

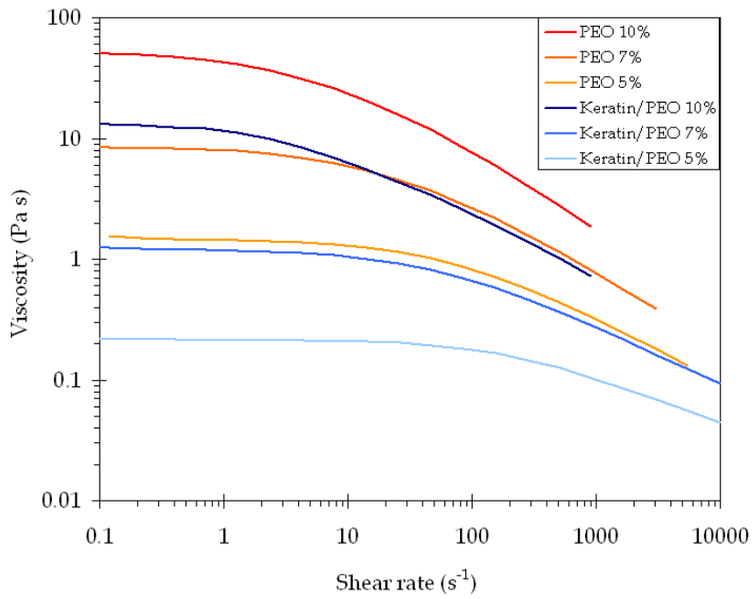

Fig. 5. Viscosity flow curves of PEO and keratin/PEO solutions

4.3 Electrospinning and morphological study

Morphologies of the electrospun materials from PEO and keratin/PEO solutions were investigated for comparison. The samples were produced by varying flow-rate, voltage and polymer concentrations.

PEO nanofibres without defects were produced from the 7% wt solution at 0.01 ml min^{-1} flow-rate from 20 to 30 kV of voltage. For higher flow-rate (0.05 ml min^{-1}) macroscopic drops fall from the capillary also at the highest voltage (30 kV). The electrospinning of 5% wt solution produced nanofibres without defects using a flow-rate of 0.01 ml min^{-1} with the voltage range from 13 to 30 kV. Increasing the flow-rate to 0.03 ml min^{-1} the nanofibres became more irregular with some beads due to the insufficient stretching of the jet at voltages below 25 kV. For higher flow-rate (0.05 ml min^{-1}), the process started only at 30 kV; whereas at lower voltages the solution dripped from the capillary.

Nanofibres of keratin/PEO blend with regular diameter distribution and few defects were electrospun from the solutions at 7 and 10 % wt of polymers concentration applying a

voltage from 20 to 30 kV and a solution flow-rate of 0.01 ml min^{-1} (Fig. 6 a). The keratin/PEO solutions at high concentrations (7 and 10 % wt) produce fibres with few defects, like 5 and 7 % wt PEO solutions, probably because they have a similar flow behaviour. At low polymers concentration (5 % wt) the nanofibres were electrospun with many defects also at high voltage (25-30 kV), as Fig. 6 b shows, and the solution dripped from the capillary during the process at voltages below 20 kV because of the low viscosity.

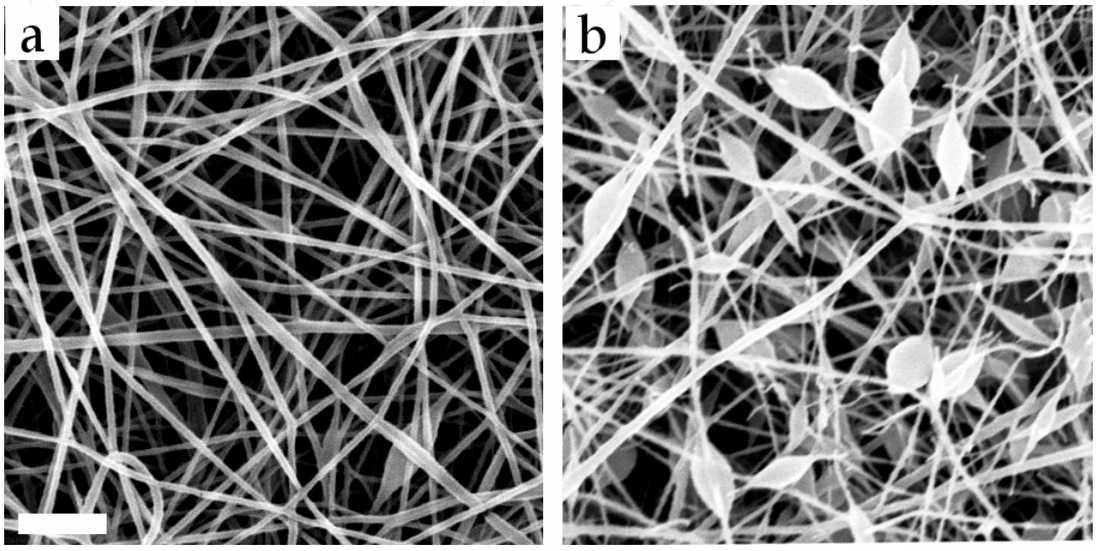

Fig. 6. Electrospun nanofibres of 50/50 keratin/PEO blend at 25 kV, 0.01 ml min^{-1} from (a) 7 % wt and (b) 5 % wt solutions. Scale bar = 2 μm.

The average diameters of the electrospun nanofibres, measured at 150 different points from SEM pictures for each sample produced, as a function of the applied voltage. The diameters of the nanofibres produced at the same voltage from 5 and 7 % wt of pure PEO solutions are generally comparable. The keratin/PEO solution produces nanofibres with small diameter at higher voltage (30 kV), whereas at 20 kV electrospun nanofibres have a diameter much higher than the pure PEO nanofibres at the same voltage. Moreover, the slope of the diameter/voltage trend-line for the keratin/PEO blend is the highest obtained in our experiment (Aluigi et al., 2007b). Thus, it seems that the presence of keratin strengthens the influence of the voltage on the size of the filaments. Since the keratin has many different functional groups, it is possible that inter- and intra-molecular bonds increase the jet rigidity when the solvent evaporates. Therefore, a higher voltage is required to stretch the solidifying keratin/PEO solution jet.

4.4 Thermal analysis

The DSC curves of electrospun keratin/PEO samples, compared with the films produced by casting from the same solution, are shown in Fig. 7 with the aim of highlighting the structural changes induced by the electrospinning process.

The endothermic overlapped peaks at around 60°C are due to the fusion of PEO crystalline phase and to the evaporation of water, especially absorbed by keratin. It is worth noting that in the keratin/PEO film, the water evaporation occurs at lower temperature with respect to keratin/PEO nanofibres (50°C in the nanofibres and 80°C in the film). This is probably due

to the high surface/volume ratio of the nanofibres which promotes water evaporation even at lower temperatures.
The DSC analysis the electrospun PEO exhibits a slight increase of the melting point. It is believed that the high stretching due to the electrospinning process promotes the orientation of the long polymer chains of PEO. This high degree of order shifts the melting point to a higher temperature.
The endothermic events observed in the range of 200-350°C are attributed to protein denaturation followed by protein degradation (Spei & Holzem, 1990). The thermograms show that the peaks related to the protein denaturation, which falls at 233°C in the film, shifts to lower temperature (213°C) in the electrospun sample. It could be presumed that the high draw, given by electrospinning process, and the quick water evaporation hinders the keratin self-assembly leading the protein chains to assume a less complex supermolecular organization which denatures at lower temperatures. This thermal behaviour is in agreement with the FT-IR observations (Aluigi et al., 2007b); in fact, the keratin in the electrospun fibres shows a molecular conformation characterized by weaker hydrogen bonds that make the protein less thermally stable.

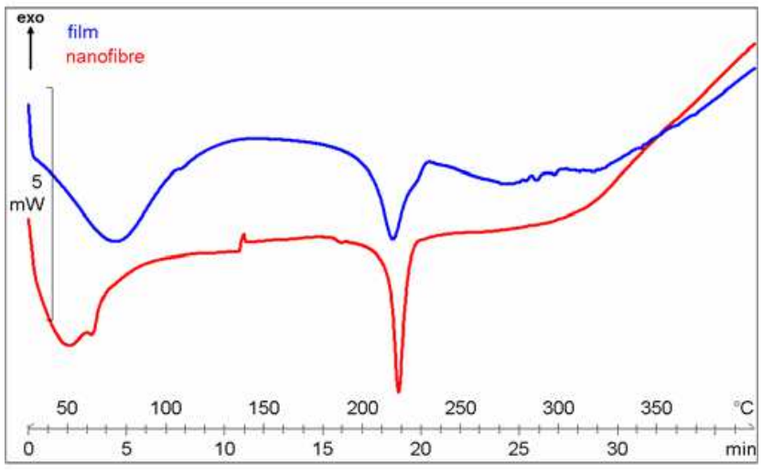

Fig. 7. DSC analysis of keratin/PEO film from casting and keratin/PEO nanofibres from electrospinning.

5. Keratin/PA6 blend nanofibres

Since mid-1990s, there has been an increasing interest in the application of nano-sized fibres for high efficiency filtration (Montefusco, 2005; Gopal et al., 2006; Dotti et al., 2007). Indeed, high surface area associated to great surface cohesion and small pore dimensions of nanofibrous mats allow the capture of submicron particles improving filtration efficiency, cleaning operations and filter life. As far as "active" filtration is concerned, keratin is a bio-polymer that can absorb and remove toxic, sensitizing and suspected carcinogenic agents substances such as heavy-metal ions (copper, chromium, lead, mercury, etc.) (Kar & Misra, 2004; Ki et al., 2007; Aluigi et al., 2009), formaldehyde (Wortmann et al., 1999) and other hazardous VOCs.
Keratin is rich in amino acids having polar and ionisable side chains able to bind charged species such as metal ions. In particular, having a pK_a about 4.5, free carboxyl groups of

aspartyl and glutamyl residues are considered the most likely binding sites over a wide pH range (Maclaren & Milligan, 1981; Taddei et al., 2003). Recent studies showed that formic acid is a good media to dissolve keratin having strong solvation properties for keratin regenerated from wool (Alemdar et al., 2005; Aluigi et al., 2007a). Formic acid is also a solvent for polyamides so that it can be used to prepare keratin-polyamide 6 (PA6) blends in different proportions.

5.1 Solution characterizations

Keratin/PA6 blend solutions with different blending ratios (100/0, 90/10, 70/30, 50/50, 30/70, 10/90 and 0/100), prepared by mixing solutions at 15% wt of pure keratin and pure PA6 separately dissolved in concentrated formic acid, can be processed into nanofibres by electrospinning, with different results according to viscosity and conductivity of the solutions. Viscosities measured at the shear rate 84 s^{-1} show deviation from linearity when compared with the theoretical values calculated by the additive rule (Eq. 2):

$$\ln \eta_T = \sum_i w_i \ln \eta_i \tag{2}$$

where: w_i is the weight fraction of the i^{th} component, η_i is the solution viscosity of the i^{th} component and η_T is the theoretical viscosity of the polymer blend. The fitting of the experimental measurements displays a negative deviation from the additive rule indicating a negligible interaction between the protein and the synthetic polymer. Moreover, viscosity of the blend solutions decreased with increasing the keratin content, while electrical conductivity (about of 2 mS cm^{-1}) did not change significantly.

5.2 Electrospinning and morphological study

Electrospinning is successful at room temperature, 25 kV applied voltage, 0.01 ml min^{-1} flow rate and 10 cm working distance, producing very thin nanofibres in the range from 70 to 300 nm, with mean diameter of about 150 nm.

SEM images of the nanofibres with different compositions randomly deposited on the collecting screen are shown in Fig. 8. Nanofibres obtained by electrospinning keratin/PA6 blends are thin and free from defects, but pure keratin nanofibres show many bead defects since the jet breaks up into droplets as a result of the lower viscosity of the solution. The mean diameter of the nanofibres does not change significantly with the blend composition; however, nanofibres rich in PA6 appear more homogeneous than keratin rich ones.

5.3 Testing and characterization

Chemical interactions between the polymers can be excluded, according to the viscosity measurements and by the study of FT-IR spectra in the region 4000–2600 cm^{-1} and 2000-900 cm^{-1}. Indeed, the nanofibre blend spectra appear as weighed overlapped spectra of pure keratin and pure PA6; a broadening of the Amide A and Amide I bands can be observed with increasing the keratin content and also the intensity of the 1025 cm^{-1} peak (Bunte salt) increases with increasing the keratin content. But the absence of both band shifts and new peaks exclude chemical interaction.

The nanofibres containing more than 50% wt of keratin, are totally destroyed due to swelling of regenerated keratin when it contacts with water. On the other hand, morphology doesn't change for pure PA6 and keratin/PA6 10/90 nanofibres while those of keratin/PA6

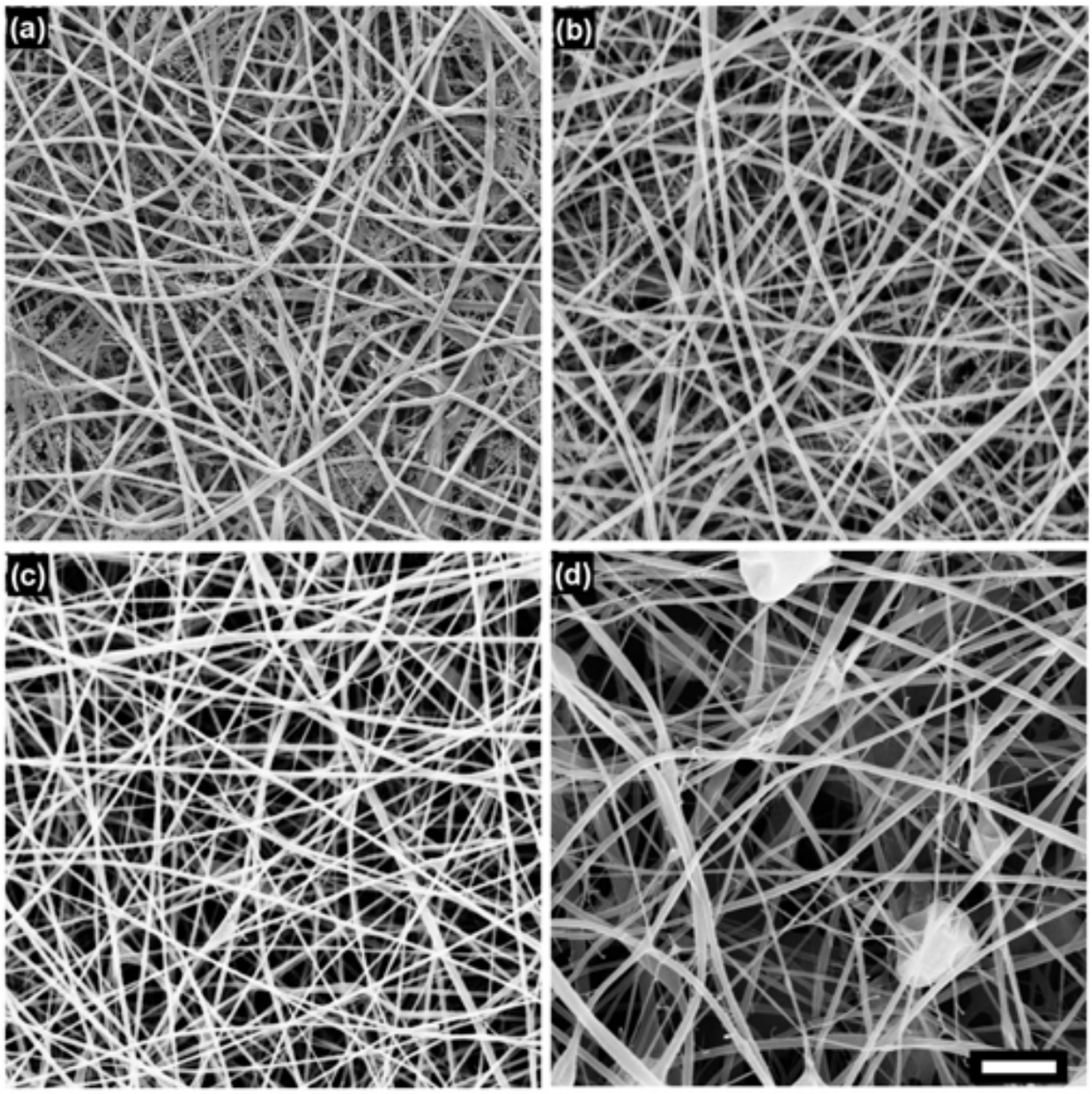

Fig. 8. Keratin/PA6 blend nanofibres: (a) 30% keratin, (b) 70% keratin, (c) 90% keratin and (d) pure keratin. Scale bar = 2 μm.

30/70 start swelling and become flat. The adsorption of Cr^{3+} ions by keratin can be studied only at low pH values in order to avoid the precipitation of chromium hydroxide above pH 4 (Maclaren & Milligan, 1981). Cr^{3+} uptake of pure PA6 and blend nanofibres was calculated using the following Eq. 3:

$$q\ (\mu\text{g/mg}) = \frac{q_0 - q_1}{m} \tag{3}$$

where q_0 and q_1 are the Cr^{3+} amount (μg) in the 10 ml of standard solution before and after adsorption, respectively, and m is the mass of the nanofibres. The Cr^{3+} adsorption of keratin/PA6 0/100, 10/90 and 30/70 nanofibres were compared with that of blend films obtained by casting from the same solutions. The chromium uptake of the nanofibres

slightly increases with the increasing the keratin content. Moreover, the adsorption capacity of the nanofibrous mats is much higher than that of films with the same composition, since the higher surface area of the nanofibres increases the number of available binding sites. Both films and nanofibrous membranes were cut into square shapes of 4 cm^2 and placed in a standard solution (10 ml) of chromium ions, with an initial concentration of 50 μg/L at pH 4, for 24 hours. The standard solution was prepared diluting with deionised water a stock solution of chromium (III) nitrate nonahydrate in nitric acid 1000 μg/ml. The Cr^{3+} concentration of the solution after immersion of the nanofibre mats was analysed by a Atomic Adsorption Spectrometer. Before the measurements, the calibration curve was made using standard solution of Cr^{3+} at 25, 50, 75 and 100 μg l^{-1}.

For the formaldehyde adsorption tests, multi-component filters of polypropylene (PP) and keratin/PA6 blend nanofibres were prepared by electrospinning the blend solutions directly onto the surface of the polypropylene filters. Adsorption tests were carried out using an apparatus composed as follows: a closed chamber having a volume of 3.3 L, a fan forcing air to pass through the filter, a filter holder and a Formaldemeter™ htV (PPM Technology Ltd.). About 0.6 ppm of formaldehyde was introduced in the chamber by using formaldehyde-releasing silica. When a stable concentration was reached in the chamber, the solid was removed, the multi-component filter was introduced in the chamber and the measurement started. The adsorption tests were performed at 20°C and 65% R.H. measuring the formaldehyde concentration versus time. The adsorption of gases on solid surfaces includes physiosorption and chemisorption. The physiosorption occurs when the interaction forces between adsorbent and adsorbate are intermolecular attractions (Van der Waals forces), while the chemisorption is a type of adsorption whereby the adsorbent adheres to the adsorbate through the formation of chemical bonds. Therefore, chemisorption is more selective than physiosoprtion.

It is known that formaldehyde has high reactivity towards proteins; in fact it is able to react with different side chains of amino acids such as the amino groups of lysine, arginine,

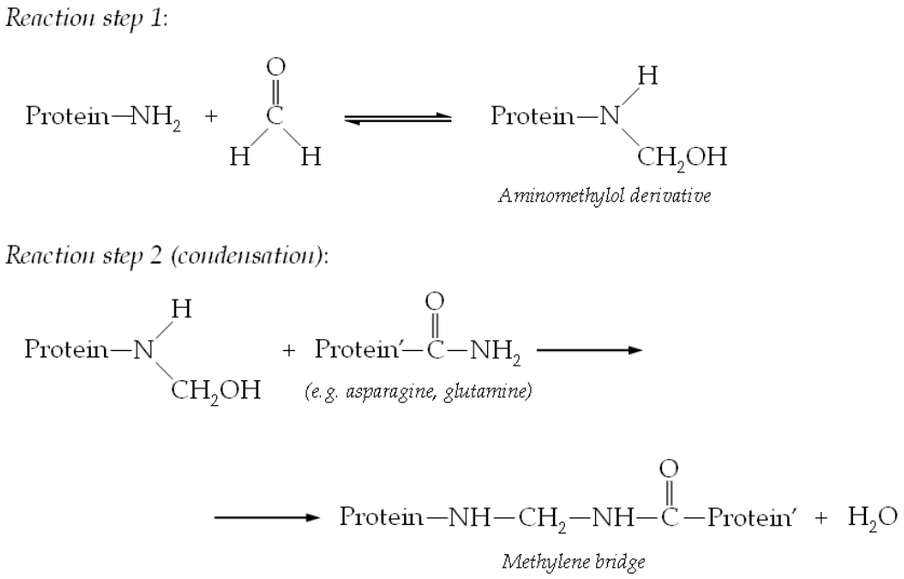

Fig. 9. Reaction scheme of formaldehyde with keratin proteins

glutamine and asparagine. The reaction scheme is reported in Fig. 9. The first reaction step involves amino groups and formaldehyde and produces an unstable product (aminomethylol derivative). The second reaction leads to a stable methylene bridge (Wortmann et al., 2005).
The adsorption performances of keratin-based nanofibres were compared with that of PP filters and pure PA6 nanofibres/PP filters. Because of the selectivity of keratin towards formaldehyde, only the nanofibres containing the 90% wt of keratin were studied. It was found that PP filters and multi-component filters of PP sheets and PA6 nanofibres can reduce the formaldehyde concentration of about 30% and 40% respectively, but the reduction reaches 70% in the presence of keratin based nanofibres. The main reason is that PP and PA6 nanofibres/PP filters adsorb formaldehyde only by physiosorption. On the other hand keratin based nanofibres have stronger capability of adsorbing formaldehyde because in the adsorbing process both physiosorption and chemisorption occur simultaneously.

6. Research trends

In the biomedical field great efforts have recently been made to mimic nature by producing nanofibrous materials solely composed of natural polymers in the assumption that such materials would be less subject to rejection by the host. Moreover, electrospinning of natural proteins offers a promising method to produce nanofibres with a similar nanofibrillar structure to that of a native extra-cellular matrix. Unfortunately, the electrospinning of natural macromolecules has demonstrated to be a challenge because they frequently do not possess the viscoelastic properties needed for good electrospinning. One exception is silk fibroin, a natural high molecular weight polypeptide. Silk fibroin is spun by *Bombix mori* and can be extracted in two molecular weights: 25 kDa (light chains) and 320–390 kDa (heavy chains). Silk fibroin is rich in glycine, alanine and serine amino acids. In the last years, regenerated silk fibroin has been proposed for the fabrication of a variety of biomaterials such as films, sponges, gels and fibres for biomedical applications.
Recently, keratin/fibroin blend has received much attention due to their potential applications in tissue engineering (Vasconcelos et al., 2008), and also for removal of metal ions and water purification (Ki et al., 2007; Baek et al., 2007).
Keratin/fibroin blended materials are a totally protein material (biodegradable and natural) that could combine the interesting properties of keratin (VOCs and metal ion adsorption) with the mechanical properties and electrospinnability of silk fibroin. Moreover, synergic effects could enhance some properties: for instance, it was found that films cast from silk fibroin and keratin decreased blood coagulation compared with silk fibroin or keratin alone (Lee et al., 1998).
Concerning the production of keratin/fibroin nanofibres by electrospinning, both silk fibroin and wool keratin can be dissolved in formic acid and mixed in several blending ratios (Ki et al., 2007; Baek et al., 2007; Zoccola et al., 2008). Blend nanofibers rich in fibroin, show branched and flatten morphology characterized by a bimodal diameter distribution. In spite of the lower viscosities of the solutions, nanofibers rich in keratin have more homogeneous diameter distribution, with a round cross section. This may be due to the higher conductivity that promotes nanofiber formation. Keratin rich nanofibers are also thinner than those rich in fibroin.

Particular behaviour was observed for the 50/50 blend solutions that showed the highest zero-shear viscosity and the longest relaxation time (i.e. lowest shear thinning onset). The resulting nanofibers were thin with respect to those produced with the other blend ratios, and the trend was repeated at different operating conditions (Zoccola et al., 2008). It had been supposed some interactions between keratin and fibroin promote the formation of entangled chain networks. It has also been pointed out that keratin/fibroin 50/50 blend nanofibers have excellent mechanical properties (Baek et al., 2007). These studies encourage further investigations into these types of natural matrices for use in the biomedical field, biotechnology and water purification.

7. References

Alemdar, A.; Iridag, Y. & Kazanci, M. (2005). Flow behavior of regenerated wool-keratin proteins in different mediums. *International Journal of Biological Macromolecules.*, 35, 151-153.

Aluigi, A.; Innocenti, R.; Tonin, C. & Vineis, C. (2004). Studies on keratin/cellulose films from cuprammonium solution. *Autex Research Journal*, 4, 175-181.

Aluigi, A.; Zoccola, M.; Vineis, C.; Tonin, C.; Ferrero, F. & Canetti, M. (2007a). Study on the structure and properties of wool keratin regenerated from formic acid. *International Journal of Biological Macromolecules.*, 41, 266-273.

Aluigi, A.; Varesano, A.; Montarsolo, A.; Vineis, C.; Ferrero, F; Mazzuchetti, G. & Tonin, C. (2007b). Electrospinning of keratin/PEO blend nanofibres. *Journal of Applied Polymer Science*, 104, 863-870.

Aluigi, A.; Vineis, C.; Varesano, A.; Mazzuchetti, G.; Ferrero, F. & Tonin, C. (2008). Structure and properties of keratin/PEO blend nanofibres. *European Polymer Journal*, 44, 2465-2475.

Aluigi, A.; Vineis, C.; Tonin, C.; Tonetti, C.; Varesano, A. & Mazzuchetti, G. (2009). Wool keratin-based nanofibres for active filtration of air and water. *Journal of Biobased Materials and Bioenergy*, 3, 311–319.

Baek, D.H.; Ki, C.S.; Um, I.C. & Park, Y.H. (2007). Metal ion adsorbability of electrospun wool keratose/silk fibroin blend nanofiber mats. *Fibers and Polymers*, 8, 271-277.

Barhate, R.S. & Ramakrishna, S. (2007). Nanofibrous filtering media: filtration problems and solutions from tiny materials. *Journal of Membrane Science*, 296, 1–8.

Barone, J.R.; Schmidt, W.F. & Liebner, C.F (2005). Thermally processed keratin films. *Journal of Applied Polymer Science*, 97, 1644-1651.

Bergsma, J.E.; Rozema, F.R.; Bos, R.R.M.; de Bruijn, W.C.; Boering, G. & Pennings, A.J. (1995). In vivo degradation and biocompatibility study of in vitro pre-degraded as-polymerized polylactide particles. *Biomaterials*, 16, 267–274.

Bryner M. & Armantrout, J. (2006). *U.S. Patent* 2006138710.

Cecil, R. (1963). In: *The proteins*, Vol. 1, Neurath H. (Ed.), Academic Press, New York, USA.

Cooley, J.F. (1902). *U.S. Patent* 692631.

Crick, F.H.C. (1953). The Fourier transform of a coiled-coil. *Acta Crystographica*, 6, 685-689.

Deitzel, J.M.; Kleinmeyer, J.; Hirvonen, J.K. & Beck Tan, N.C. (2001). Controlled deposition of electrospun poly(ethylene oxide) fibers. *Polymer*, 42, 8163–8170.

Desai, N.P. & Hubbel, J.A. (1991). Solution technique to incorporate polyethylene oxide and other water-soluble polymers into surfaces of polymeric biomaterials. *Biomaterials*, 12, 144–153.

Dotti, F.; Varesano, A.; Montarsolo, A.; Aluigi, A; Tonin, C. & Mazzuchetti, G. (2007). Electrospun porous mats for high efficiency filtration. *Journal of Industrial Textiles*, 37, 151-162.

Dowling, L.M.; Crewther, W.G. & Parry, D.A.D. (1986). Secondary structure of component 8c-1 of α-keratin. *Biochemical Journal*, 236, 705-712.

Ellison, C.J.; Phatak, A.; Giles, D.W.; Macosko, C.W. & Bates, F.S. (2007). Melt blown nanofibers: fiber diameter distributions and onset of fiber break-up. *Polymer*, 48, 3306–3316.

Formhals, A. (1934). *U.S. Patent* 1975504.

Fraser, R.D.B.; MacRae, T.P.; Parry, D.A.D. & Suzuki, E. (1971). The structure of feather keratin. *Polymer*, 12, 35-56.

Fraser, R.D.B.; MacRae, T.P. & Rogers, G.E. (1972). In: *Keratins: Their composition, structure and biosynthesis*, Charles C. Thomas Publisher, Springfield, Illinois, USA.

Furth, M.E.; Atala, A. & Van Dyke, M.E. (2007). Smart biomaterials design for tissue engineering and regenerative medicine. *Biomaterials*, 28, 5068-5073.

Garret, R.H. & Grisham, C.M. (2002). In: *Biochemistry 2nd Edition*, Higher Education Press, Beijing, China.

Gibson, P.; Schreuder-Gibson, H. & Rivin, D. (2001). Transport properties of porous membranes based on electrospun nanofibers. *Colloid Surface A*, 187–188, 469–481.

Gopal, R.; Kaur, S.; Ma, Z.; Chan, C.; Ramakrishna, S. & Matsuura, T. (2006). Electrospun nanofibrous filtration membrane. *Journal of Membrane Science*, 281, 581–586.

Hamasaki, S.; Tachinaba, A.; Tada, D.; Yamauchi, K. & Tanabe, T. (2008). Fabrication of highly porous keratin sponges by freeze-drying in the presence of calcium alginate beads. *Material Science and Engineering: C*, 28, 1250-1254.

Homonoff, E. (2008). Nanofibrillated fibers: opening newmarkets to nanofibre usage. *International Fibers Journal* 23, 22–24.

Huang, Z.M.; Zhang, Y.Z.; Kotaki, M. & Ramakrishna, S. (2003). A review on polymer nanofibers by electrospinning and their applications in nanocomposites. *Composites Science Technology*, 63, 2223–2253.

Jeffrey, P.D. (1972). The molecular weights of the low-sulphur proteins from wool: A review. *Journal of the Textile Institute*, 63, 91-113.

Jin, H.J.; Fridrikh, S.V.; Rutledge, G.C. & Kaplan, D.L. (2002). Electrospinning Bombyx mori silk with poly(ethylene oxide). *Biomacromolecules*, 3, 1233–1239.

Kar, P. & Misra, M. (2004). Use of keratin fiber for separation of heavy metals from water. *Journal of Chemical Technology & Biotechnology*, 79, 1313-1319.

Katoh, K.; Shibayama, M.; Tanabe, T. & Yamauchi, K. (2004). Preparation and properties of keratin-poly(vinyl alcohol) blend fiber. *Journal of Applied Polymer Science*, 91, 756-762.

Ki, C.S.; Gang, E.H.; Um, I.C. & Park, Y.H. (2007). Nanofibous membrane of wool keratose/silk fibroin blend for heavy metal ion adsorption. *Journal of Membrane Science*, 302, 20-26.

Kilic, A.; Oruc, F. & Demir, A. (2008). Effects of polarity on electrospinning process. *Textile Research Journal*, 78, 532–539.

Lee, K.; Kong, S.; Park, W.; Ha, W. & Kwon, I. (1998). Effect of surface properties on the antithrombogenicity of silk fibroin/S-carboxymethyl kerateine blend films. *Journal of Biomaterial Science Polymer Edition*, 9, 905-914

Lee, J.; Cuddihy, M.J. & Kotov, N.A. (2008). Three-dimensional cell culture matrices: State of the art. *Tissue Engineering B*, 14, 61–86.

Li, D. & Xia, Y. (2004). Electrospinning of nanofibers: reinventing the wheel. *Advanced Materials*, 16, 1151–1170.

Li, L.; Frey, M.W. & Green, T.B. (2006). Modification of air filter media with nylon-6 nanofibers. *Journal of Engineered Fibers and Fabrics*, 1, 1–24.

Maclaren, J.A. & Milligan, B. (1981). The chemical reactivity of the wool fibre, In: *Wool science*, pp. 109-127, Science Press, Marrickville, Australia.

Martínez-Hernández, A.L.; Velasco-Santos, C.; De-Icaz, M. & Castaño, V.M. (2007). Dynamical–mechanical and thermal analysis of polymeric composites reinforced with keratin biofibers from chicken feathers. *Composites Part B: Engineering*, 38, 405-410.

Montefusco F. (2005). The use of nonwovens in air filtration. *Filtration and Separation*, 42, 30-31.

Morton, W.J. (1902). *U.S. Patent* 705691.

Pauling, L. & Corey, R.B. (1953). Compound helical configurations of polypeptide chains: Structure of proteins of the α-keratin type. *Nature*, 171, 59-61.

Perez, M.; Swan, M. & Louks, J. (2000). *U.S. Patent* 6110588.

Pham, Q.P.; Sharma, U. & Mikos, A.G. (2006). Electrospinning of polymeric nanofibers for tissue engineering applications: A review. *Tissue Engineering*, 12, 1197–1211.

Pourdeyhimi, B.; Fedorova, N. & Sharp, S. (2006). *U.S. Patent* 2006292355.

Qin, X.H. & Wang, S.Y. (2006). Filtration properties of electrospinning nanofibers. *Journal of Applied Polymer Science*, 102, 1285–1290.

Ramakrishna, S.; Fujihara, K.; Teo, W.E.; Yong, T.; Ma, Z. & Ramaseshan, R. (2006). Electrospun nanofibers: Solving global issues. *Materials Today*, 9, 40–50.

Reneker, D.H. & Yarin, A.L. (2008). Electrospinning jets and polymer nanofibers. *Polymer*, 49, 2387-2425.

Schmidt, W.F. (1998). Innovative feather utilization strategies, *Proceedings of the National Poultry Waste Management Symposium*, pp. 276-282, Springdale, AR, October 19-22, 1998.

Schrooyen, P.M.M.; Dijkstra, P.J.; Oberthür, R.C.; Bantjes, A. & Feijen J. (2001). Stabilization of solutions of feather keratins by sodium dodecyl sulfate. *Journal of Colloid and Interface Science*, 240, 30-39.

Shenoy, S.L.; Bates, W.D.; Frisch, H.L. & Wnek, G.E. (2005). Role of chain entanglements on fiber formation during electrospinning of polymer solutions: good solvent, non-specific polymer–polymer interaction limit. *Polymer*, 46, 3372-3384.

Shin, Y.M.; Hohman, M.M.; Brenner, M.P. & Rutledge, G.C. (2001). Experimental characterization of electrospinning: the electrically forced jet and instabilities. *Polymer*, 42, 9955–9967.

Shin, C.; Chase, G.G. & Reneker, D.H. (2005). The effect of nanofibers on liquid–liquid coalescence filter performance. *AIChE Journal*, 51, 3109–3113.

Sill, T.J. & von Recum, H.A. (2008). Electrospinning: Applications in drug delivery and tissue engineering. *Biomaterials*, 29, 1989-2006.

Son, W.K.; Youk, J.H.; Lee, T.S. & Park W.H. (2004). The effects of solution properties and polyelectrolyte on electrospinning of ultrafine poly(ethylene oxide) fibers. *Polymer*. 45, 2959-2966.

Spei, M. & Holzem, R. (1990). Further thermoanalytical investigations of annealed keratins: The time and temperature dependence. *Colloid and Polymer Science*, 268, 630-635.

Tachinaba, A.; Furuta, Y.; Takeshima, H.; Tanabe, T. & Yamauchi, K. (2002). Fabrication of wool keratin sponge scaffolds for long-term cell cultivation. *Journal of Biotechnology*, 93, 165-170.

Tachinaba, A.; Kaneko, S.; Tanabe, T. & Yamauchi, K. (2005). Rapid fabrication of keratin–hydroxyapatite hybrid sponges toward osteoblast cultivation and differentiation. *Biomaterials*, 26, 297-302.

Taddei, P.; Monti, P.; Freddi, G.; Arai, T. & Tsukada, M. (2003). Binding of Co(II) and Cu(II) cations to chemically modified wool fibres: An IR investigation. *Journal of Molecular Structure*, 650, 105-113.

Tanabe, T.; Okitsu, N. & Yamauchi, K. (2004). Fabrication and characterization of chemically crosslinked keratin films. *Materials Science and Engineering: C*, 24, 441–446.

Theron, S.A.; Zussman, E. & Yarin, A.L. (2004). Experimental investigation of the governing parameters in the electrospinning of polymer solutions. *Polymer*, 45, 2017–2030.

Thompson, E.O.P. & O'Donnel I.J. (1959). Studies on oxidized wool: A comparison of the completeness of oxidation with peracetic and performic acids. *Australian Journal of Biological Sciences*, 12 282-292.

Tonin, C.; Aluigi, A.; Bianchetto Songia, M.; D'Arrigo, C.; Mormino, M. & Vineis, C. (2004). Thermoanalytical characterization of modified keratin fibres. *Journal of Thermal Analalysi and Calorimetry*, 77, 987-996.

Tonin, C.; Zoccola, M.; Aluigi, A.; Varesano, A.; Montarsolo, A.; Vineis, C. & Zimbardi, F. (2006). Study on the conversion of wool keratin by steam explosion. *Biomacromolecules*, 7, 3499-3504.

Tsai, P.P.; Schreuder-Gibson, H. & Gibson, P. (2002). Different electrostatic methods for making electret filters. *Journal of Electrostatics*, 54, 333–341.

Tseng, A.A.; Notargiacomo, A. & Chen, T.P. (2005). Nanofabrication by scanning probe microscope lithography: A review. *Journal of Vacuum Science and Technology B*, 23, 877–894.

Varesano, A.; Aluigi, A.; Vineis, C. & Tonin, C. (2008). Study on the shear viscosity behaviour of keratin/PEO blends for nanofibre electrospinning. *Journal of Polymer Science Part B: Polymer Physics*, 46, 1193-1201.

Vasconcelos, A.; Freddi, G. & Cavaco-Paulo, A. (2008). Biodegradable materials based on silk fibroin and keratin. *Biomacromolecules*, 9, 1299-1305.

von Bergen, W. (1963). In: *Wool Handbook 3rd Edition*, Vol. 1, John Wiley & Sons, Inc., New York, USA.

Wortmann, G.; Zwiener, G.; Sweredjiuk, R.; Doppelmayer, F. & Wortmann, F.J. (1999). Sorption of indoor air pollutants by sheep's wool: Formaldehyde as an example. *Proceedings of the International Wool Textile Organization*, Report CTF 3, Florence, Italy, June 1999.

Wortmann, G.; Thome, S.; Sweredjuk, R. & Zwiener, G. (2005). Chemisorption of protein reactive indoor air pollutants by wool, *Proceedings of the International Wool Textile Organization Conference*, Report CTF03, pp. 1-7, Hobart, Australia, April 2005.

Xie, H.; Li, S. & Zhang, S. (2001). Ionic liquids as novel solvents for the dissolution and blending of wool keratin fibres. *Green Chemistry*, 7, 606-608.

Xie, X.N.; Chung, H.J.; Sow, C.H. & Wee, A.T.S. (2006). Nanoscale materials patterning and engineering by atomic force microscopy nanolithography. *Materials Science and Engineering R: Reports*, 54, 1–48.

Yamauchi K.; Yamauchi A.; Kusunoki T.; Kohda A. & Konishi Y. (1996) Preparation of stable aqueous solution of keratins and physiochemical and biodegradational properties of films. *Journal of Biomedical Material Research*, 31, 439-444.

Yarin, A.L.; Koombhongse, S. & Reneker, D.H. (2001). Taylor cone and jetting from liquid droplets in electrospinning of nanofibers. *Journal of Applied Physics*, 90, 4836–4846.

Yin, J.; Rastogi, S.; Terry, A.E. & Popescu, C. (2007). Self-organization of oligopeptides obtained on dissolution of feather keratins in superheated water. *Biomacromolecules*, 8, 800-806.

Zhang, S. (2002). Emerging biological materials through molecular self-assembly. *Biotechnology Advances*, 20, 321–339.

Zoccola, M.; Aluigi, A.; Vineis, C.; Ferrero, F.; Piacentino, M. & Tonin, C. (2008). Study on cast membranes and electrospun nanofibers made from keratin/fibroin blends. *Biomacromolecules*, 9, 2819-2825.

Nanofibers

Edited by Ashok Kumar

ISBN 978-953-7619-86-2
Hard cover, 438 pages
Publisher InTech
Published online 01, February, 2010
Published in print edition February, 2010

“There’s Plenty of Room at the Bottom” this was the title of the lecture Prof. Richard Feynman delivered at California Institute of Technology on December 29, 1959 at the American Physical Society meeting. He considered the possibility to manipulate matter on an atomic scale. Indeed, the design and controllable synthesis of nanomaterials have attracted much attention because of their distinctive geometries and novel physical and chemical properties. For the last two decades nano-scaled materials in the form of nanofibers, nanoparticles, nanotubes, nanoclays, nanorods, nanodisks, nanoribbons, nanowhiskers etc. have been investigated with increased interest due to their enormous advantages, such as large surface area and active surface sites. Among all nanostructures, nanofibers have attracted tremendous interest in nanotechnology and biomedical engineering owing to the ease of controllable production processes, low pore size and superior mechanical properties for a range of applications in diverse areas such as catalysis, sensors, medicine, pharmacy, drug delivery, tissue engineering, filtration, textile, adhesive, aerospace, capacitors, transistors, battery separators, energy storage, fuel cells, information technology, photonic structures and flat panel displays, just to mention a few. Nanofibers are continuous filaments of generally less than about 1000 nm diameters. Nanofibers of a variety of cellulose and non-cellulose based materials can be produced by a variety of techniques such as phase separation, self assembly, drawing, melt fibrillation, template synthesis, electro-spinning, and solution spinning. They reduce the handling problems mostly associated with the nanoparticles. Nanoparticles can agglomerate and form clusters, whereas nanofibers form a mesh that stays intact even after regeneration. The present book is a result of contributions of experts from international scientific community working in different areas and types of nanofibers. The book thoroughly covers latest topics on different varieties of nanofibers. It provides an up-to-date insightful coverage to the synthesis, characterization, functional properties and potential device applications of nanofibers in specialized areas. We hope that this book will prove to be timely and thought provoking and will serve as a valuable reference for researchers working in different areas of nanofibers. Special thanks goes to the authors for their valuable contributions.

How to reference

In order to correctly reference this scholarly work, feel free to copy and paste the following:

Claudio Tonin, Annalisa Aluigi, Alessio Varesano and Claudia Vineis (2010). Keratin-based Nanofibres, Nanofibers, Ashok Kumar (Ed.), ISBN: 978-953-7619-86-2, InTech, Available from: http://www.intechopen.com/books/nanofibers/keratin-based-nanofibres

InTech Europe
University Campus STeP Ri
Slavka Krautzeka 83/A
51000 Rijeka, Croatia
Phone: +385 (51) 770 447
Fax: +385 (51) 686 166
www.intechopen.com

InTech China
Unit 405, Office Block, Hotel Equatorial Shanghai
No.65, Yan An Road (West), Shanghai, 200040, China
中国上海市延安西路65号上海国际贵都大饭店办公楼405单元
Phone: +86-21-62489820
Fax: +86-21-62489821

IntechOpen

IntechOpen